Voltage Imbalance Compensation for Droop-Controlled Inverters in Islanded Microgrid

Amin Ranjabaran*[1] , Mahmoud Ebadian[2], Mohammad Sadegh Ghazizadeh[3]

[1]Department of Electrical and Electronics Engineering, Islamic Azad university, Gonabad Branch,Gonabad, Iran,amranjbaran@gmail.com
[2]Department of Electrical and Computer Engineering, University of Birjand, Birjand, Iran, mahmoud_ebadian@birjand.ac.ir
[3]Department of Electrical and Computer Engineering, Abbaspour College, Shahid Beheshti University, Tehran, Iran, ghazizadeh@pwut.ac.ir

Abstract

In this paper, a new control strategy is proposed for implementation in low-voltage microgrids with balanced/ unbalanced load circumstances. The proposed scheme contains, the power droop controllers, inner voltage and current loops, the virtual impedance loop, the voltage imbalance compensation. The proposed strategy balances the voltage of the single-phase critical loads by compensating the imbalanced voltage drop on the feeders. In addition, this strategy has also shown to be capable of restoring critical loads' voltage to nominal values .This method also shares the real and reactive load accurately between DG units, based on their capacity. The simulation results in MATLAB /SIMULINK environment show the efficiency of the proposed approach in improving power sharing among DG units and decreasing voltage imbalance

1. Introduction

A typical AC microgrid system comprises of DG units like photovoltaic generation, wind generation, fuel cell generation, energy storage systems and distributed load with inverters and incorporate control systems. The DG units usually are in DC form or have middle DC bus, that connected to AC bus through voltage source inverters(VSIs)[1, 2]. The main task of a VSI is to control the power injected by the DG[3]. Therefore, by employing appropriate control techniques, these inverters can also be used for compensating voltage imbalance.

A microgrid may inherently be subjected to significant degrees of imbalance conditions due to the presence of single-phase loads[4]. The imbalanced voltage has noticeable negative influences on critical loads are sensitive to voltage deviations[5]. Therefore, a control strategy should be designed for the DG units to improve the performance of microgrids under imbalanced loading conditions. One major method for compensation of voltage imbalance and harmonics is the use of series active power filter in series with the distribution line by injecting negative sequence

and harmonic voltage [6]. Also, in [7, 8], shunt compensation is provided to mitigate voltage imbalanced and harmonic distortion. In this method, imbalanced load voltage is compensated by balancing the line currents. However, for the islanded microgrid conditions, it is uneconomic to install extra series/parallels active power filter for each of the DG. In [9], a control scheme has been proposed for compensating the microgrid voltage imbalance. This scheme compensates the voltage imbalance at the DG output. The drawback of this method is the imbalanced voltage at the PCC (point of common coupling) is not compensated. In [10], droop control method is improved through online virtual impedance adjustment to address inaccurate power sharing problems. In [11], the virtual negative-sequence impedance controller is proposed to effectively compensate the negative-sequence currents of the imbalanced loads. Furthermore, several control strategies have been presented to improve the quality of ac microgrid[12, 13]. In [14] a control strategy based on droop control is proposed for a microgrid. The method improves the power quality and proper

power sharing in the presence of imbalanced and nonlinear loads. In[15, 16], the virtual impedance is proposed to balance load voltage. To consider the voltage imbalance compensation at the critical load bus, a distributed cooperative control scheme is proposed in [17] and a hierarchical control structure for voltage quality enhancement in microgrid is proposed in [18]. The limitation of this method is costly when the number of DGs becomes larger and larger. Furthermore, in most proposed methods, power quality problems under imbalanced loads and power sharing problems with mismatch feeder impedance are scarcely considered.In order to realize accurate power sharing among DG units while also ensure voltage imbalance compensation, this paper proposes a novel control strategy for an islanded microgrid, which uses communication links to balance and restore the PCC voltage amplitude. In this control strategy, the voltage reference for each DG unit is generated by the P-f/Q-V droop method. In order to avoid the real and reactive power control coupling and also, due to the accuracy of sharing between the DG units, the virtual impedance loop with voltage and current control loops have been utilized. In this strategy, in order to balance the PCC voltage, the voltage drop between the DG's output and PCC has been estimated for each phase and added to the voltage reference generated by the Q-V droop control. Moreover, the Low Bandwidth Communication (LBC) has been used to transmit the data information of the Energy Management System (EMS) to local controllers of DG units. The EMS calculates the power reference values based on the total load.

2. Traditional Droop Control

The droop control method can be studied by considering an equivalent circuit of a DG connected to load bus, as shown in Fig 1. The DG unit modeled as an AC source, with the voltage of $V_S \angle \delta$. The load bus voltage is $V_L \angle 0$.
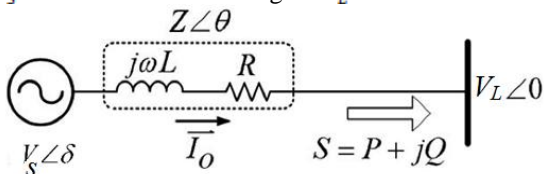

Fig. 1.   Equivalent circuit of a DG connected to a load bus.

The real and reactive power delivered to load bus is given by

$$P = \frac{V_S^2}{Z} \cos\theta - \frac{V_S V_L}{Z} \cos(\theta + \delta) \qquad (1)$$

$$Q = \frac{V_S^2}{Z} \sin\theta - \frac{V_S V_L}{Z} \sin(\theta + \delta) \qquad (1)$$

If the effective line impedance is purely inductive, $\theta = 90^o$ and $Z = jX$, then (1), (2) can be reduce to

$$P = \frac{V_S V_L}{X} \sin(\delta) \qquad (2)$$

$$Q = \frac{V_S^2}{X} - \frac{V_S V_L}{X} \cos(\delta) \qquad (3)$$

If the phase difference between the DG output voltage and load bus, δ, is small, it is reasonable to suppose, $\cos\delta \approx 1$ and $\sin\delta \approx \delta$. Then, the frequency and amplitude of the DG output voltage reference can be expressed as follows:

$$f = f_0 - k_p (P_0 - P) \qquad (4)$$

$$V = V_0 - k_q (Q_0 - Q) \qquad (5)$$

where f_0, V_0 are the frequency and voltage magnitude references, k_p, k_q are droop coefficients and P_0 and Q_0 represent the real and reactive power references.

3. The Proposed Control Strategy

A typical AC microgrid with DG units and balanced and imbalanced loads is shown in Fig 2. Each DG unit consists of the renewable energy source (RES), VSI and output LC filter and through a feeder is connected to the PCC. It has been supposed that DG capacities can be different. The local controllers consist of the power droop controllers, virtual impedance loop, inner voltage and current loops and the imbalance voltage compensator. The proposed control strategy in islanding mode is shown in Fig 3. It includes five different stages: (1) Calculation the real and reactive power for each phase of DG unit' output. (2) Voltage reference generation with traditional droop control method. (3) Virtual impedance loop. (4) Voltage imbalance compensation. (5) Inner voltage and current control loops.

A) *Calculation of P and Q for Each Phase*

The real and reactive power for each phase of DG unit' output has been obtained from the measured signals. For phase-a, the DG output voltage (V_{oa}) and current (I_{oa}) are used to determine the instantaneous real power (p_a) and reactive power (q_a) as a follow[19]:

$$p_a = V_{oa} I_{oa} \qquad (6)$$

$$q_a = V_{oa} I_{oa}(-90^o) \qquad (7)$$

The -90° phase shift in I_{oa} is required to calculate the reactive power. Subsequently, p_a and q_a are processed by low-pass filter(LPF) in order to obtain the filtered output real and reactive powers.

Similarly, for phase b and c, the instantaneous real and reactive power can be calculated for each
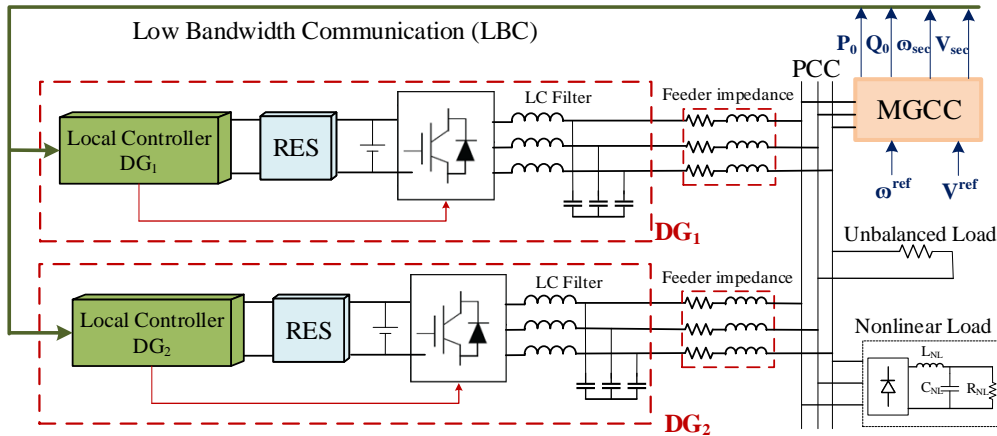
phase, separately.

Fig. 2.   A typical AC microgrid with communication links to a EMS.

B) *The P-f/Q-V droop control*

The voltage references of VSI (voltage source inverter) by P-f/Q-V droop control defined as follows:

$$f = f_0 - D_p[P_0 - (P_a + P_b + P_c)] \qquad (8)$$

$$V = V_0 - D_q[Q_0 - (Q_a + Q_b + Q_c)] \qquad (9)$$

The P_0, Q_0 from each DG are set by the EMS.

C) *Voltage Imbalance Compensation*

Under the imbalanced loading conditions, power consumption of the single-phase loads in microgrid systems will not be identical and hence; currents flow in each phase will be different. In traditional droop control method, DG output voltage is balanced, due to the presence of imbalanced voltage drop on the feeder, PCC voltage will be imbalanced. Therefore, in this paper, the voltage drop between the DG's output and PCC has been estimated for each phase and added to voltage reference generated by the Q-V droop control method, which will lead to a balanced PCC voltage. Furthermore, this method can improve accuracy reactive power sharing, which affect by the feeder impedance mismatch. If resistance and reactance of the feeder impedances are not the same, the voltage drop on the feeder are not equal and accuracy reactive power sharing is reduced. But, with proposed control method, the voltage drop mismatch is compensated.
The Eq. (4) can be represented by

$$Q = \frac{V_S(V_S - V_L)}{X} = \frac{V_S \Delta V}{X} \qquad (10)$$

$$\frac{\Delta V}{Q} = \frac{X}{V_S} \qquad (11)$$

Therefore, there is linear relevance between the DG output reactive power and the voltage magnitude difference (between DG output voltage and PCC voltage). This linear relevance can be expressed as[20]

$$K_Q = \frac{\Delta V}{Q} = \frac{X}{V_S} \qquad (12)$$

where ΔV, Q are the DG output voltage magnitude difference and the DG output reactive power, respectively .As presented in (13), the K_Q is related to the system voltage, and the inductance between the DG output and the PCC. The inductance is often not readily available. Therefore, this coefficient(K_Q) must be estimated without the knowledge of the feeder impedance. According to Eq. (10), if reactive power output of the DG with the reactive power reference (Q_0) is equal, so, the DG output voltage and the voltage magnitude reference (V_0) will be equal. Therefore, the difference between the DG output voltage and PCC voltage is actually the PI controller's output ($Q_0 - Q$). The $\Delta V/Q$ coefficient can be achieved as ($K_Q = (Q_0 - Q)/Q_0$). A LPF is used to smoothen the achieved coefficient (K_Q), which is subsequently applied to estimate the voltage drop across feeder impedance between the output DG and PCC. The reactive power reference from each DG has been set by the EMS. The assigned powers are transmitted to the DG unit's local controllers. Therefore, the phase-a voltage drop across the feeder impedance is presented as follows:

$$\Delta V_a = K_Q \cdot Q_a \qquad (13)$$

where Q_a is the phase-a output reactive power of DG unit i.

Similarly, the voltage drop on the feeder for phase-b and phase-c can also be calculated.

$$\Delta V_b = K_Q . Q_b \tag{14}$$

$$\Delta V_c = K_Q . Q_c \tag{15}$$

Finally, the voltage drops have been added to the reference voltage achieved by the Q-V droop control method.

D) *Virtual impedance loop*

In the presented paper, the virtual impedance is considered to enhance the performance of the droop controllers. The inductive part contributes in reducing the circulating current and decoupling control of the real and reactive power, and the resistive part improves the system damping[21].The voltage drop of the virtual impedance in αβ axis are derived as

$$V_{v\alpha} + jV_{v\beta} = (R_v + j\omega L_v)(i_{0\alpha} + j i_{o\beta})$$

$$V_{v\alpha} = R_v . i_{0\alpha} - \omega L_v i_{0\beta} \tag{16}$$

$$V_{v\beta} = R_v . i_{0\beta} + \omega L_v i_{0\alpha} \tag{17}$$

where R_v and L_v are the virtual resistance and inductance values, respectively.

E) *Inner voltage and current control loops*

The voltage and current control loops are based on stationary reference frame, and the proportional-resonant controller (PR) is used. The transfer function of the PR controller can be given by[22]

$$G_V(s) = k_{pv} + \frac{2k_{iv}\,\omega_c s}{s^2 + 2\omega_c s + \omega_0{}^2} \tag{18}$$

$$G_i(s) = k_{pi} + \frac{2k_{iI}\,\omega_c s}{s^2 + 2\omega_c s + \omega_0{}^2} \tag{19}$$

where k_{pv} and k_{pi} are the proportional gains, k_{iv} and k_{iI} represent the resonant gains term and ω_c the cut-off frequency for resonant bandwidth control.

F) *Controller designed and parameter determination*

The block diagram of the voltage and current controls for the quadrature axes α and β, with additional virtual impedance (without imbalance compensation) has been shown in Fig 4.
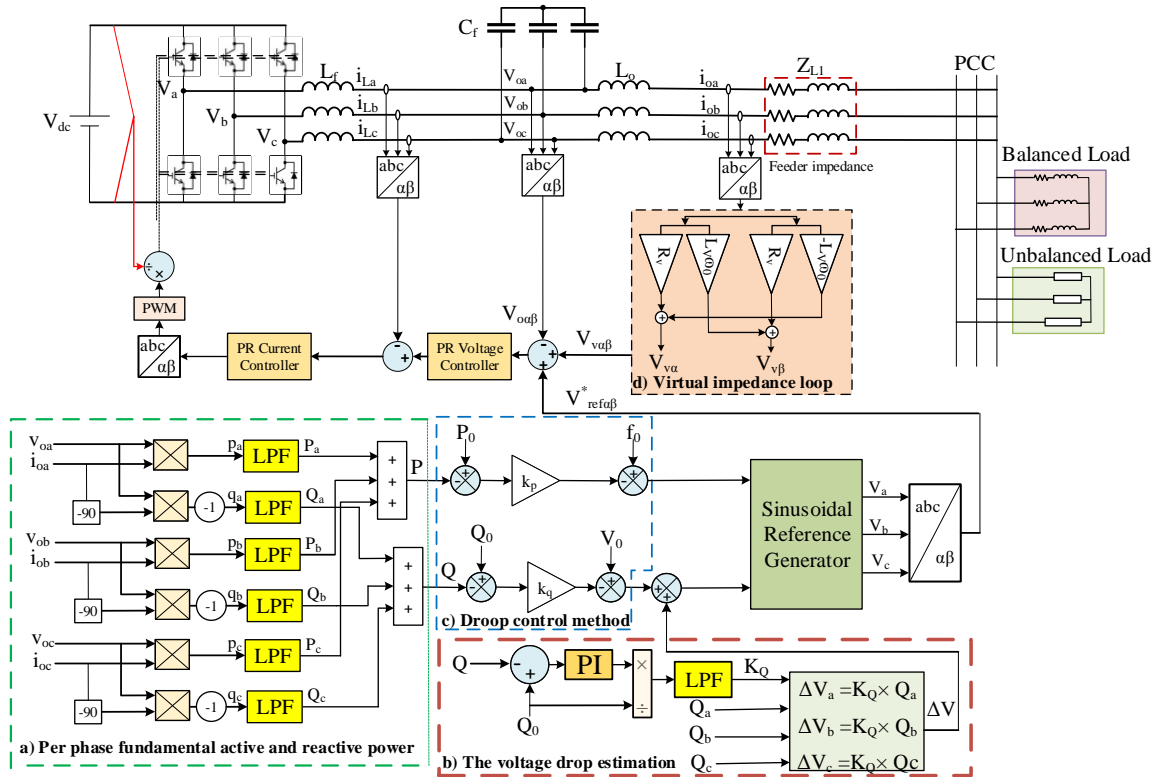

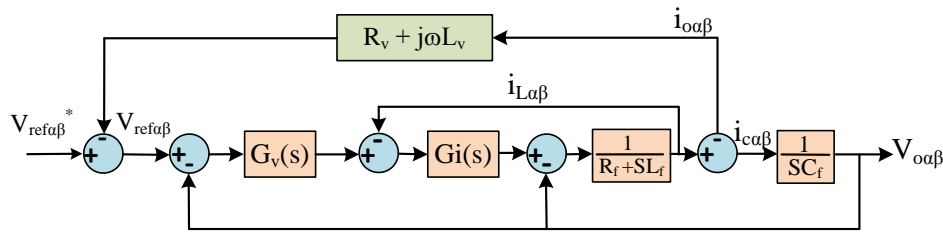Fig. 3.   Block diagram of the proposed voltage control strategy

Fig. 4.   Blok diagram of the inner loops with virtual impedance.

The closed-loop transfer function of the inner loops can be expressed by:

$$V_{o\alpha\beta}(s) = \frac{G_i(s)G_v(s)Z_c}{Z_c + Z_f + G_i(s) + G_i(s)G_v(s)Z_c}V_{ref\alpha\beta}(s)$$

$$-\frac{Z_c(G_i(s)+Z_f)}{Z_c + Z_f + G_i(s) + G_i(s)G_v(s)Z_c}i_{o\alpha\beta}(s) \qquad (2$$

where $Z_f(s)=R_f + sL_f$ and $Z_c(s) = 1/sC_f$. The closed loop transfer function of the inner loops can be simply expressed by:

$$V_{o\alpha\beta}(s) = G(s)V_{ref\alpha\beta}(s) - Z_o(s)i_{o\alpha\beta}(s) \qquad (21)$$

where $G(s)$ is the voltage gain transfer function and $Z_o(s)$ is the output impedance of the inverter. The voltage loop reference signals are modified via the virtual impedance loop. Therefore, the output voltage of a DG unit can be derived as

$$V_{o\alpha\beta}(s) = G(s)V_{ref\alpha\beta}(s) - (G(s)Z_v(s)+Z_o(s))i_{o\alpha\beta}(s) \ (22)$$

The total output impedance of the DG is defined as

$$Z_t(s) = \frac{V_{o\alpha\beta}(s)}{i_{o\alpha\beta}(s)}\bigg|_{V_{ref\alpha\beta}(s)=0} \qquad (23)$$

The total output impedance of the inverter, with virtual impedance loop, can be derived:

$$Z_t(s) = G(s)Z_v(s) + Z_{o\alpha\beta}(s) \qquad (24)$$

The bode plots of the closed-loop voltage gain and output impedance have been presented in Fig 5. with the system parameters and controller parameters given in Table 1. Based on Fig 5, it can be seen that the magnitude and phase angle of the closed-loop voltage gain at the fundamental frequency (50 Hz) are about 1 dB and 0, respectively. So, the voltage loop obtains the zero-error tracking capability at the fundamental frequency[23].

4. Simulation Results

In order to verify the effectiveness of the proposed control strategy, a microgrid with two DG units has been chosen, which the rating DG1 is twice that of DG2, and shown by Fig 6. The detailed system parameters are shown in Table 1, it can be observed that the value of the feeder impedance Z2 is considered to be twice that of the feeder impedance Z1. A balanced load with Y connection plus imbalanced loads (three single-phase loads) are connected to the PCC for consideration of voltage imbalance conditions. The real and reactive power load in each phase has been illustrated in Table 2. The load of phase-c has been categorized as a sensitive type. In this paper, all the three-phase waveforms shown by the colors blue, red and green represent phase-a, phase-b and phase-c, respectively. The RMS values of PCC voltage using the proposed control strategy and traditional droop control have been presented by Fig. 7. This can be seen in Fig 7(a), that the PCC voltage has been reduced using traditional droop control, accordingly, the PCC voltage from the phase-a and phase-b is at about 221 volts, while the critical load voltage connected to phase-c is around 212 volts. According to Fig 7(b), it is clear that the RMS values of the PCC voltage close to the nominal value have been set. The details of the voltage unbalance factor (VUF) calculation are illustrated in Fig 8. As shown in Fig. 9(a), the VUF of the PCC voltage with traditional droop control method is about 1.5%, whereas the proposed control strategy shows values about 0.06%. As a result, PCC voltage imbalance is decreased, while the DG voltage output becomes imbalanced. Furthermore, because of the less feeder impedance of DG_1; its VUF has increased a little more.

In order to illustrate unbalance compensation more clearly, the three-phase voltage and current waveforms from DG_1 and DG_2 terminal and output voltages at PCC have been compared with the proposed scheme and traditional droop control (Figs 10 and 11). Power demand of critical loads at phase-c is greater than other two phases, which results in a higher current level as well. In traditional droop control method, the output voltage of DG units is balanced. Therefore, due to the rather high rate of current at phase-c, the voltage drop across feeder impedance of phase-c will be greater and lead to a lower PCC voltage from this phase in comparison to other phases, as shown by Fig 10(c).

Bode Diagram

(a)
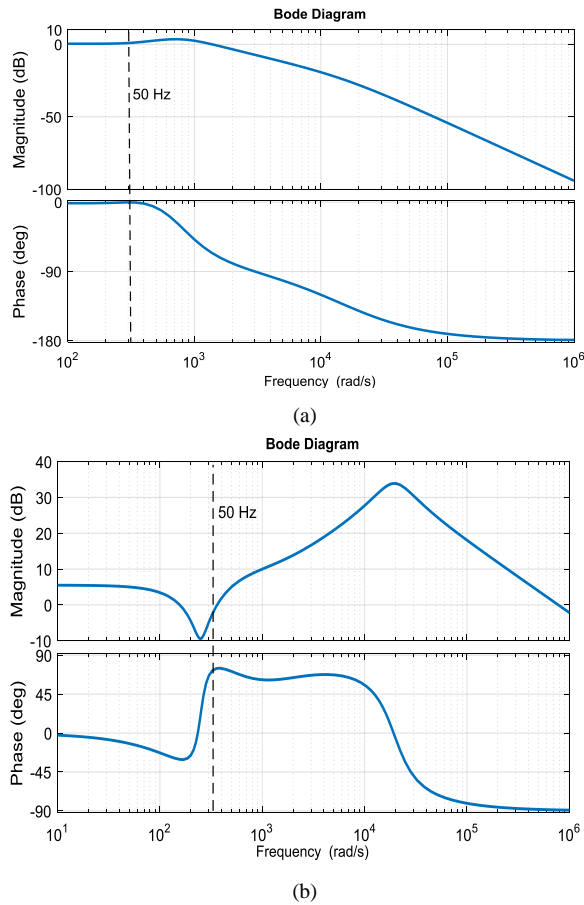
Bode Diagram

(b)

Fig. 5.   Bode diagram of the closed-loop voltage gain and output impedance of a DG unit. (a) Closed-loop voltage gain with PR controller. (b) The output impedance with virtual impedance loop.

However, by using the voltage drop estimation of the feeder impedance for each phase separately, and the addition to the reference voltage generated by the Q-V droop control method, PCC voltage has been balanced and set at nominal values, without balancing phase currents. The waveforms of the balanced PCC voltages have been illustrated by Fig 11(c). These Figs demonstrate the effectiveness of the proposed compensation method in balancing out PCC voltages. In Fig 12, the real and reactive power sharing among DG units with proposed control strategy has been shown. As previously mentioned, the capacity of the DG_1 is twice DG_2. It can be observed in Fig 13, by proposed control strategy, the real and reactive powers are properly shared among DG units based on their capacity, and the amount of the Q_1 supplied by DG_1 is accurately twice of the supplied by DG_2.

5. Conclusion

A control strategy for the PCC voltage imbalance compensation in an islanded microgrid has been proposed, tested, and compared to traditional droop control method. The proposed

strategy contains the power droop controllers, inner voltage and current loops, the virtual impedance loop and the imbalance voltage compensator. In this proposed control strategy, the droop control generates the voltage references for DG units. The voltage imbalance compensator estimates the voltage drop on the feeder for each phase, without knowledge of feeder impedance. Also, the virtual impedance loop has been utilized for real and reactive power decoupling. The proposed strategy has been validated through simulation results. The obtained result shows that the PCC voltage imbalanced is compensated and restored to nominal value, while real and reactive powers are shared properly between DG units.
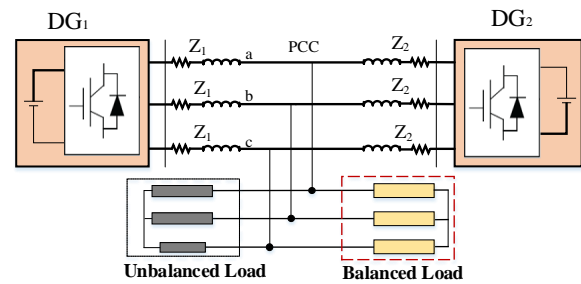

Fig. 6.   Islanded microgrid with two DGs and imbalanced load.

Table.1.
System parameters in simulation

System parameter	Value
DC link voltage	650
Main grid	400 V (line to line RMS) /50 Hz
LC filter	$L_f = 8$ mH , $C_f = 50$ μF
k_p , k_q	0.001rad/s/W, 0.0001 V/Var
R_{v1} , L_{v1}	0.2 Ω , 2 mH
R_{v2} , L_{V2}	0.4 Ω , 4 mH
Z_1	2+j0.565 Ω
Z_2	4+j1.31 Ω
k_{pv}	0. 55
k_{iv}	35.5
k_{pI}	30
k_{iI}	1000
$_f\omega$	10 rad/s
$_c\omega$	5 rad/s

Table.2.
The real and reactive power of each phase of the load

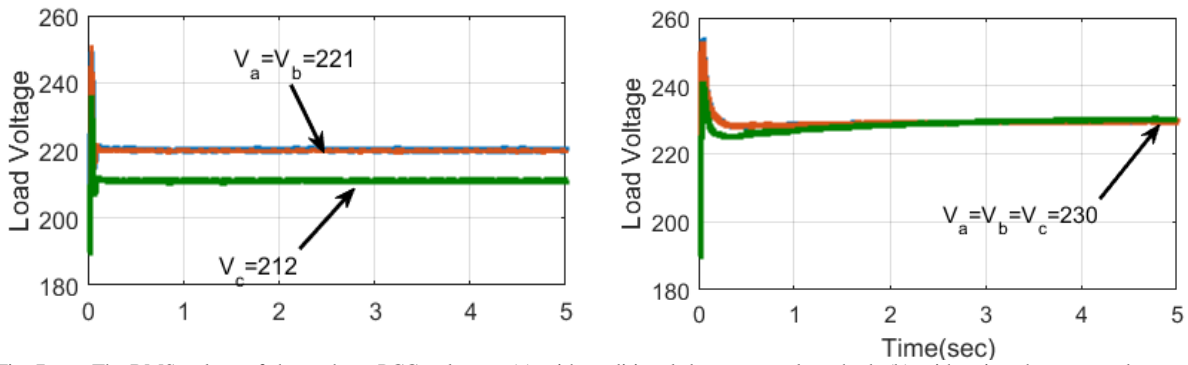| Power of the three loads		Load of the phase-a	Load of the phase-b	Load of the phase-c
Balanced load	Real and reactive power	1000 W, 300 Var	1000 W, 300 Var	1000 W, 300 Var
Imbalanced load	Real and reactive power	800 W, 200 Var	800 W, 200 Var	2400 W, 600 Var

Fig. 7.   The RMS values of three-phase PCC voltages. (a) with traditional droop control method. (b) with using the proposed control method.
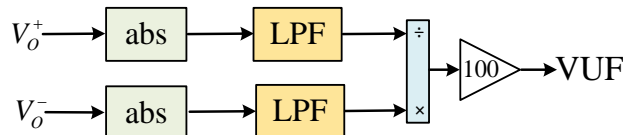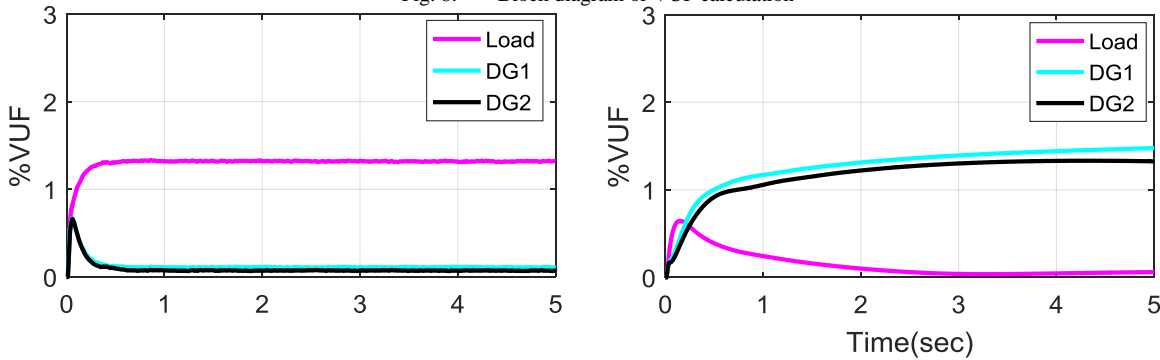

Fig. 8.   Block diagram of VUF calculation

Fig. 9.   VUF at load and DGs output. (a) with traditional droop control method. (b) with using the proposed control strategy.

(a)   (b)   (c)

(d)   (e)   (f)
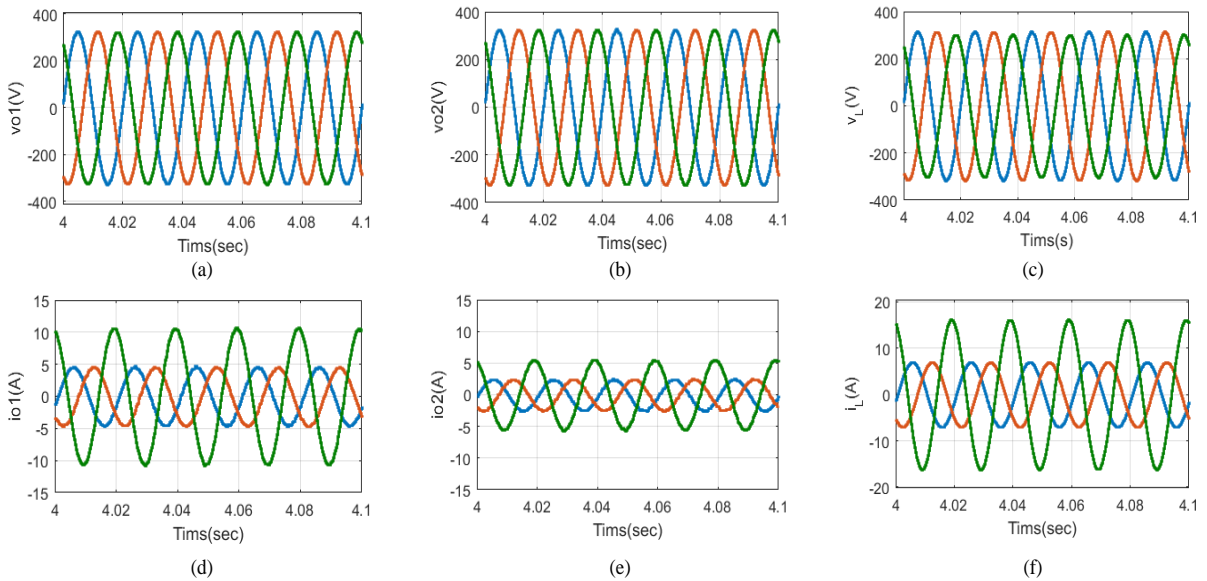
Fig. 10.   Results of the microgrid system with traditional droop control method. (a) output voltage of DG1 (b) output voltage of DG2 (c)PCC voltage (d)output current of DG1 (e)output currnt of DG2. (f)PCC currents
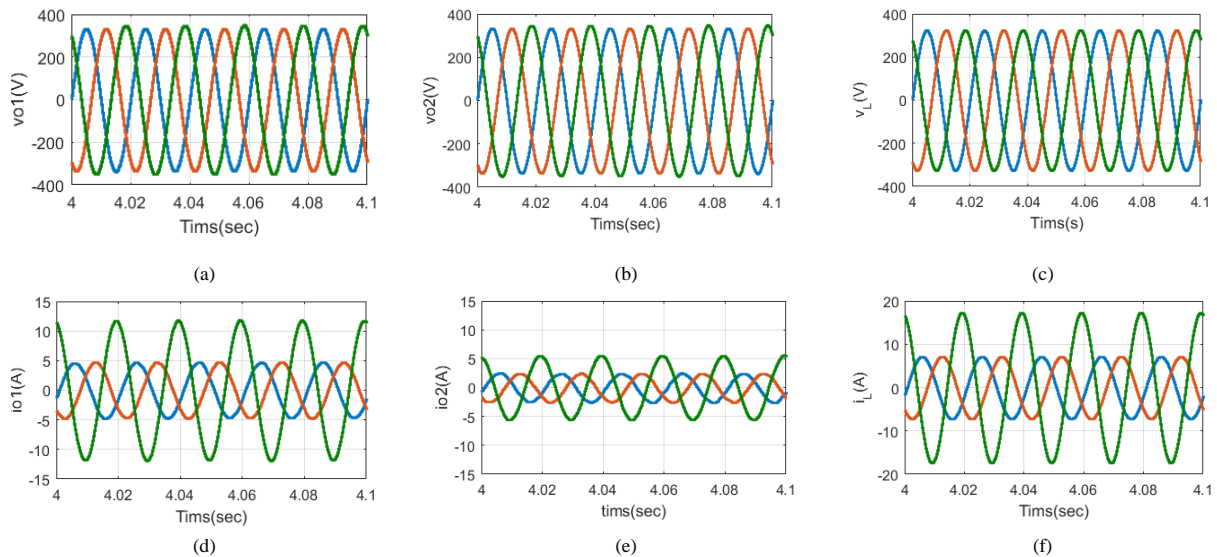
Fig. 11.   Results of the microgrid system using with proposed control system (a) output voltage of DG1 (b) output voltage of DG2 (c)PCC voltage (d)output current of DG1 (e)output currnt of DG2. (f)PCC currents
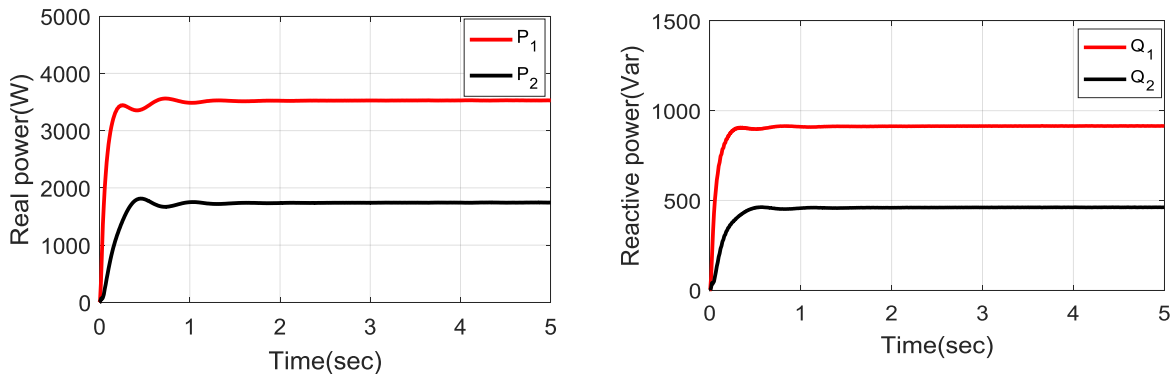

Fig. 12.   Power sharing performance with proposed control strategy. (a) Real power. (b) Reactive power.

References

[1]   J. Rocabert, A. Luna, F. Blaabjerg, and P. Rodriguez, "Control of power converters in AC microgrids," Power Electronics, IEEE Transactions on, vol. 27, no. 11 , 2012.

[1]   J. M. Guerrero, F. Blaabjerg, T. Zhelev, K. Hemmes, E. Monmasson, S. Jemei, M. P. Comech, R. Granadino, and J. I. Frau, "Distributed generation: Toward a new energy paradigm," IEEE Industrial Electronics Magazine, vol. 4, no. 1, 2010.

[2]   R. Asad, and A. Kazemi, "A novel decentralized voltage control method for direct current microgrids with sensitive loads," International Transactions on Electrical Energy Systems, vol. 25, no. 2, 2015.

[3]   M. Hamzeh, S. Emamian, H. Karimi, and J. Mahseredjian, "Robust Control of an Islanded Microgrid Under Unbalanced and Nonlinear Load Conditions," IEEE Journal of Emerging and Selected Topics in Power Electronics, vol. 4, no. 2 , 2016.

[4]   A. Von Jouanne, and B. Banerjee, "Assessment of voltage unbalance," IEEE transactions on power delivery, vol. 16, no. 4 , 2001.

[5]   M. S. Hamad, M. I. Masoud, and B. W. Williams, "Medium-voltage 12-pulse converter: output voltage harmonic compensation using a series APF," IEEE Transactions on Industrial Electronics, vol. 61, no. 1 , 2014.

[6]   [7]   A. Garcia-Cerrada, O. Pinzon-Ardila, V. Feliu-Batlle, P. Roncero-Sánchez, and P. García-González, "Application of a repetitive controller for a three-phase active power filter," IEEE Transactions on Power Electronics, vol. 22, no. 1 , 2007.

[7]   A. Masmoudi, S. Piasecki, M. Jasiński, and A. Milicua, "Brief view on control of grid-interfacing AC-DC-AC converter and active filter under unbalanced and distorted voltage conditions," COMPEL-The international journal for computation and mathematics in electrical and electronic engineering, vol. 30, no. 1, 2011.

[8]   M. Savaghebi, A. Jalilian, J. C. Vasquez, and J. M. Guerrero, "Secondary Control Scheme for Voltage Unbalance Compensation in an Islanded Droop-Controlled Microgrid," Smart Grid, IEEE Transactions on, vol. 3, no. 2, 2012.

[9]   J. He, Y. W. Li, and F. Blaabjerg, "An Enhanced Islanding Microgrid Reactive Power, Imbalance Power, and Harmonic Power Sharing Scheme," Power Electronics, IEEE Transactions on, vol. 30, no. 6 , 2015.

[10] M. Hamzeh, H. Karimi, H. Mokhtari, and J. Mahseredjian, "Control of a microgrid with unbalanced loads using virtual negative-sequence impedance loop."

[11] Y. Li, D. M. Vilathgamuwa, and P. C. Loh, "Microgrid power quality enhancement using a three-phase four-wire

grid-interfacing compensator," IEEE Transactions on Industry Applications, vol. 41, no. 6, 2005.

[12] Y. W. Li, D. M. Vilathgamuwa, and P. C. Loh, "A grid-interfacing power quality compensator for three-phase three-wire microgrid applications."

[13] R. Majumder, A. Ghosh, G. Ledwich, and F. Zare, "Load sharing and power quality enhanced operation of a distributed microgrid," IET Renewable Power Generation, vol. 3, no. 2, 2009.

[14] M. Savaghebi, J. C. Vasquez, A. Jalilian, J. M. Guerrero, and T. L. Lee, "Selective harmonic virtual impedance for voltage source inverters with LCL filter in microgrids."

[15] X. Wang, F. Blaabjerg, and Z. Chen, "Autonomous control of inverter-interfaced distributed generation units for harmonic current filtering and resonance damping in an islanded microgrid," IEEE Transactions on Industry Applications, vol. 50, no. 1, 2014.

[16] F. Guo, C. Wen, J. Mao, J. Chen, and Y. D. Song, "Distributed Cooperative Secondary Control for Voltage Unbalance Compensation in an Islanded Microgrid," IEEE Transactions on Industrial Informatics, vol. 11, no. 5, 2015.

[17] M. Savaghebi, A. Jalilian, J. C. Vasquez, and J. M. Guerrero, "Secondary control for voltage quality enhancement in microgrids," IEEE Transactions on Smart Grid, vol. 3, no. 4 , 2012.

[18] D. De, and V. Ramanarayanan, "Decentralized Parallel Operation of Inverters Sharing Unbalanced and Nonlinear Loads," IEEE Transactions on Power Electronics, vol. 25, no. 12, 2010.

[19] L. Yun Wei, and K. Ching-Nan, "An Accurate Power Control Strategy for Power-Electronics-Interfaced Distributed Generation Units Operating in a Low-Voltage Multibus Microgrid," Power Electronics, IEEE Transactions on, vol. 24, no. 12, 2009.

[20] J. He, and Y. W. Li, "Analysis and design of interfacing inverter output virtual impedance in a low voltage microgrid."

[21] A. Hasanzadeh, O. C. Onar, H. Mokhtari, and A. Khaligh, "A proportional-resonant controller-based wireless control strategy with a reduced number of sensors for parallel-operated UPSs," IEEE Transactions on Power Delivery, vol. 25, no. 1, 2010.

[22] Q. Liu, Y. Tao, X. Liu, Y. Deng, and X. He, "Voltage unbalance and harmonics compensation for islanded microgrid inverters," IET Power Electronics, vol. 7, no. 5, 2015.